Dynamical Study of a COVID-19 Epidemic Model with Fear of Infection

[1]Usman, I. G., [2]Ibrahim, M. O., [3]Isah, B. Y., [4]Lawal, N., [5*]Akinyemi, S. T.
[1]Department of Mathematics, Zamfara State College of Education, Maru, Nigeria
[2]Department of Mathematics, University of Ilorin, Kwara State, Nigeria
[3]Department of Mathematics, Usmanu Danfodio University, Sokoto State, Nigeria
[4]Department of Veterinary Microbiology, Usmanu Danfodio University, Sokoto State, Nigeria
[5]Department of Mathematics, Sikiru Adetona College of Education, Science and Technology, Ogun State, Nigeria
*Correspondence: sammysalt047@gmail.com; akinyemist@tasce.edu.ng

D.O.I: 10.56201/ijasmt.v9.no3.2023.pg49.73

Abstract

The fear associated with an infectious disease plays a major role in the management of the infectious disease. Thus, this study tried to assess the impact of fear of infection on the spread of COVID-19 using a mathematical modelling approach. The model considered was shown to have two equilibria points, namely, the COVID-19 free equilibrium (CFE) and the COVID-19 persistent equilibrium (CPE). The computed reproduction number (R_{C1}) was used to validate the local stability of the CPE whenever R_{C1} is above one while the CFE is globally asymptotically stable $R_{C1}<1$. Next, we show that the condition $R_{C1}<1$ is sufficient to halt the spread of COVID-19 by showing that the model possesses forward bifurcation. The sensitivity analysis suggests that the fear of infection does not influence the R_{C1} while numerical simulation indicates that the population of all infected humans, COVID-19 deceased individuals and the concentration of the COVID-19 viruses in the environment increases as the fear of infection (χ_1) reduces.

Keywords: *COVID-19; Mathematical Model, Fear of Infection; Lyapunov Function; Bifurcation Analysis*

1.0 Introduction

Recently, several studies were conducted by researchers to investigate the influence of fear of the dynamics of some real-life phenomena. These areas include but are not limited to fear of crime (Benavente et al., 2023; Bove et al., 2023), fear of terrorism (Altier et al., 2023; Kaskeleviciute et al., 2023; Falcoˆ-Gimeno et al., 2023), fear of infection (Tang et al., 2023; Colonnello et al., 2023; Kroesen et al., 2023), fear of vaccination (Amanna & Slifka, 2005; Sato & Fintan, 2020; Malas et a., 2021; Bendau et al., 2021).

To gain better insight into how fear impacts the dynamics of these real-life problems, mathematical modelling is used. Terrorism model (Okoye et al., 2023), ecological models (Mondal et al., 2023; Pratama et al., 2023; Zhao & Shao, 2023), and epidemic models (Juga et al., 2021; Yousef et al., 2023; Rashid & Jarad, 2023) are some of the mathematical models that captures the impact of fear.

Murad et al. (2022), pointed out that one of the factors that affects the management of COVID-19 is the fear of being infected (Murad et al., 2022). Although the fear of the pandemic has been established by researchers to trigger various mental health issues someone who is scared of being infected may not be in a stable frame of mind (Murad et al., 2022). Apart from psychological damage caused by the pandemic, the living conditions of individuals in the populace are affected (RodrAguez-Hidalgo et al., 2020), and fear of the pandemic may weaken the public health delivery system (Shanafelt, et al., 2020). Nevertheless, there is a positive correlation between the fear of COVID-19 infection and strict compliance with preventive measures and regulations which could be beneficial to public health services (Ilesanmi & Afolabi, 2020; Murad et al., 2022; Karlsson et al., 2021; Recio-Vivas et al., 2020). Thus, the need to measure correctly the impact of fear of COVID-19 infection is of great importance to disease management.

Several mathematical models describe the spread of COVID-19 infection (Elmojtaba et al., 2023; Odetunde et al., 2022; Johnson and Pell, 2022; Thirthar et al., 2023; Usman et al., 2023). In particular, Usman et al. (2023), proposed a mathematical model that governs the transmission dynamics of COVID-19 infection coupled with the fear of infection. The proposed model was solved using the non-standard finite difference method but failed to assess the impact of fear of infection qualitatively. Thus, the goal of this paper is to study the impact of fear of infection on COVID-19 by analyzing the model presented by Usman et al. (2023) as follows:

$$\left.\begin{aligned}
\frac{dS}{dt} &= P-\Omega S-K_1S+\nu_2V\\
\frac{dV}{dt} &= \nu_1S-e\Omega V-K_2V\\
\frac{dE}{dt} &= \Omega\left(S+eV\right)-K_3E\\
\frac{dQ}{dt} &= \tau_1E-K_4Q\\
\frac{dA}{dt} &= \theta_1E-K_5A\\
\frac{dI}{dt} &= \theta_2A-K_6I\\
\frac{dH}{dt} &= \theta_3Q+\tau_2I-K_7H\\
\frac{dR}{dt} &= \alpha_1A+\alpha_2I+\alpha_3H-\mu R\\
\frac{dD}{dt} &= l_1A+l_2I+l_3H-\phi D\\
\frac{dW}{dt} &= \Pi I+\Pi\vartheta H-\varepsilon W
\end{aligned}\right\} \tag{1.1}$$

Where $S(t)$ is the unvaccinated compartment, $V(t)$ is the vaccinated susceptible compartment, $E(t)$ is the exposed compartment, $Q(t)$ is the quarantined compartment, $A(t)$ is the asymptomatic compartment, $I(t)$ is the symptomatic compartment, $H(t)$ is the hospitalized compartment, $R(t)$ is the recovered compartment, $D(t)$ is the dead compartment, $W(t)$ is the compartment for the concentration of COVID-19 viruses in the environment and

$$\Omega=\frac{\beta\left(A\eta_1+H\eta_2+W\eta_3+I\right)}{\chi_1D+1}. \tag{1.2}$$

Readers are advised to see Usman et al. (2023), for the description of parameters.

2.0 Analysis of the Model

For analysis, the following system will be considered for Model 1. Since the compartment R appears only in the eighth equation of Model 1. This implies that the remaining equation of (1.1) does not depend on the eight equations, thus it is ignored (See Makinde, 2007; Mpeshe & Nyere, 2021; Yousaf et al, 2022).

$$\frac{dS}{dt} = P - \Omega S - K_1 S + v_2 V$$
$$\frac{dV}{dt} = v_1 S - \Omega(1-b)V - K_2 V$$
$$\frac{dE}{dt} = \Omega\left(S + (1-b)V\right) - K_3 E$$
$$\frac{dQ}{dt} = \tau_1 E - K_4 Q$$
$$\frac{dA}{dt} = \theta_1 E - K_5 A$$
$$\frac{dI}{dt} = \theta_2 A - K_6 I$$
$$\frac{dH}{dt} = \theta_3 Q + \tau_2 I - K_7 H$$
$$\frac{dD}{dt} = l_1 A + l_2 I + l_3 H - \phi D$$
$$\frac{dW}{dt} = \pi I + \pi\theta H - \varepsilon W$$

(2.1)

2.1 COVID-19 Free Equilibrium

COVID-19 Free Equilibrium (CFE) points are steady-state solutions of the system (2.1) where there is no infection. Hence, in the absence of infection, $E_0, Q_0, A_0, I_0, H_0, D_0, W_0 = 0$. Then, solve the first and second equation of (2.1) for the non-infected state variables at the equilibrium point to obtain

$$S_0 = \frac{PK_2}{K_1K_2 - v_2v_1} \tag{2.2}$$

and

$$V_0 = \frac{Pv_1}{K_1K_2 - v_2v_1} \tag{2.3}$$

respectively. Thus, the disease-free equilibrium Δ_0 is given as

$$\Delta_0\left(S_0, V_0, E_0, Q_0, A_0, I_0, H_0, D_0, W_0\right) = \left(\frac{PK_2}{K_1K_2 - v_2v_1}, \frac{Pv_1}{K_1K_2 - v_2v_1}, 0, 0, 0, 0, 0, 0, 0\right)$$

(2.4)

2.2 Computation of Reproduction Number for the Model

Following the next-generation matrix method of computing the reproduction number described by Van den Driessche and Watmough (2002), the matrices for the new infection term and transfer term are respectively obtained as

$$F=\begin{pmatrix} 0 & 0 & P\beta\eta_1 A_0 & P\beta A_0 & P\beta\eta_2 A_0 & P\beta\eta_3 A_0 \\ 0 & 0 & 0 & 0 & 0 & 0 \\ 0 & 0 & 0 & 0 & 0 & 0 \\ 0 & 0 & 0 & 0 & 0 & 0 \\ 0 & 0 & 0 & 0 & 0 & 0 \\ 0 & 0 & 0 & 0 & 0 & 0 \end{pmatrix}, M=\begin{pmatrix} K_3 & 0 & 0 & 0 & 0 & 0 \\ -\tau_1 & K_4 & 0 & 0 & 0 & 0 \\ -\theta & 0 & K_5 & 0 & 0 & 0 \\ 0 & 0 & -\theta_2 & K_6 & 0 & 0 \\ 0 & -\theta_3 & 0 & -\tau_2 & K_7 & 0 \\ 0 & 0 & 0 & -\pi & -\pi\theta & \varepsilon \end{pmatrix} \tag{2.5}$$

The largest eigenvalue of the matrix FM^{-1} is computed with the aid of Maple 18 as

$$R_{C1}=\frac{P\beta A_0\left(\varepsilon K_7K_4\theta_1\left(K_6\eta_1+\theta_2\right)+\varepsilon\eta_2A_1+\pi\eta_3A_2\right)}{\varepsilon K_3K_4K_5K_6K_7} \tag{2.6}$$

where,

$$A_0=\frac{e\nu_1+K_2}{K_1K_2-\nu_2\nu_1}, A_1=K_4\tau_2\theta_1\theta_2+K_5K_6\tau_1\theta_3 \text{ and } A_2=\vartheta A_1+K_4K_7\tau_2\theta_1\theta_2 \tag{2.7}$$

The next result is valid based on Theorem 2.2 in Van den Driessche and Watmough (2002)

Lemma1: The CFE of (2.1) is locally asymptotically stable if $R_{C1}<1$ and unstable when $R_{C1}>1$.

2.3 Existence of COVID-19 Persistence Equilibrium Point

Let Δ_+ denote the COVID-19 persistence equilibrium of the model such that its component are obtained from the solution of (2.1) for $\Omega_+\neq 0$ as

$$S_+=\frac{P\left(\Omega_+e+K_2\right)}{A_5};\quad V_+=\frac{P\nu_1}{A_5};\quad E_+=\frac{P\Omega_+\left(\Omega_+e+e\nu_1+K_2\right)}{K_3A_5};$$

$$Q_+=\frac{P\Omega_+\tau_1\left(\Omega_+e+e\nu_1+K_2\right)}{K_3K_4A_5};\quad A_+=\frac{P\Omega_+\theta_1\left(\Omega_+e+e\nu_1+K_2\right)}{K_3K_5A_5};$$

$$I_+=\frac{P\Omega_+\theta_1\theta_2\left(\Omega_+e+e\nu_1+K_2\right)}{K_3K_5K_6A_5};\quad H_+=\frac{P\Omega_+A_1\left(\Omega_+e+e\nu_1+K_2\right)}{K_3K_4K_5K_6K_7A_5}$$

$$D_+ = \frac{P\Omega_+ A_4\left(\Omega_+ e + ev_1 + K_2\right)}{\phi K_3 K_4 K_5 K_6 K_7 A_5} \text{ and } W_+ = \frac{P\Omega_+ \pi A_2\left(\Omega_+ e + ev_1 + K_2\right)}{\varepsilon K_3 K_4 K_5 K_6 K_7 A_5} \tag{2.8}$$

Where $A_3 = K_4 K_7 \theta_1\left(K_6 l_1 + l_2\theta_1\right)$, $A_4 = A_3 + A_1 l_3$, and $A_5 = \Omega_+^2 e + \Omega_+\left(eK_1 + K_2\right) + K_1 K_2 - v_2 v_1$.

Substitute (2.8) into (1.2) with further simplification to get

$$a_0\Omega_+^2 + a_1\Omega_+ + a_2 = 0 \tag{2.9}$$

such that

$$a_0 = e\varepsilon\left(Px_1 A_3 + \phi K_3 K_4 K_5 K_6 K_7\right) \tag{2.10}$$

$$a_1 = \varepsilon\left(Px_1 A_3 + \phi K_3 K_4 K_5 K_6 K_7\right) - P\beta e\phi\left(\varepsilon K_7 K_4 \theta_1\left(K_6\eta_1 + \theta_2\right) + \varepsilon\eta_2 A_1 + \pi\eta_3 A_2\right) \tag{2.11}$$

$$\begin{aligned} a_2 &= e\phi K_3 K_4 K_5 K_6 K_7\left(K_1 K_2 - v_2 v_1\right) - P\beta e\phi\left(ev_1 + K_2\right)\left(\varepsilon K_7 K_4 \theta_1\left(K_6\eta_1 + \theta_2\right) + e\eta_2 A_1 + \pi\eta_3 A_2\right) \\ &= e\phi K_3 K_4 K_5 K_6 K_7\left(K_1 K_2 - v_2 v_1\right)\left(1 - R_{C1}\right) \end{aligned} \tag{2.12}$$

It is obvious from (2.10) that $a_0 > 0$ since all parameters are assumed non-negative and $a_2 < 0$ from (2.12) if $R_{C1} > 1$. Thus, according to Descarte's rule of sign, (2.9) has a unique positive root (that is COVID-19 persistent equilibrium). Hence, the following result is established.

Theorem 1. The model (2.1) has a unique COVID-19 persistent equilibrium if and only if $R_{C1} > 1$

2.5. Global Stability of CFE

Theorem 2. The COVID-19 free equilibrium of (2.1) is globally asymptotically stable if $R_{C1} < 1$, and unstable otherwise.

Proof. Following James et al. (2015) and Akinyemi et al. (2016), we consider a Lyapunov function of the form

$$f = C_1 E + C_2 Q + C_3 A + C_4 I + C_5 H + C_6 W \tag{2.13}$$

where

$$C_1 = \frac{R_C}{S_0 + eV_0}; \qquad C_2 = \frac{\beta\theta_3\left(\pi\theta\eta_3 + \varepsilon\eta_2\right)}{\varepsilon K_4 K_7}; \qquad C_4 = \frac{\beta\theta_2\left(\pi\eta_3\left(\vartheta\tau_2 + K_7\right) + \varepsilon\eta_2\tau_2 + \varepsilon K_7\right)}{\varepsilon K_6 K_7}$$

$$C_3 = \frac{\beta\left(\pi\eta_3\theta_2\left(\vartheta\tau_2 + K_7\right) + \varepsilon\eta_2\tau_2\theta_2 + \varepsilon K_7\left(\theta_2 + \eta_1 K_6\right)\right)}{\varepsilon K_4 K_6 K_7}; \qquad C_5 = \frac{\beta\left(\pi\vartheta\eta_3 + \varepsilon\eta_2\right)}{\varepsilon K_7}$$

and $C_6 \dfrac{\beta\eta_3}{\varepsilon}$ (2.14)

Differentiate (2.13) with respect to time to have

$$\frac{df}{dt} = C_1\frac{dE}{dt} + C_2\frac{dQ}{dt} + C_3\frac{dA}{dt} + C_4\frac{dI}{dt} + C_5\frac{dH}{dt} + C_6\frac{dW}{dt} \tag{2.15}$$

Substitute (2.1) into (2.15) appropriately to get

$$\frac{df}{dt} = C_1\left(\frac{\beta\left(\eta_1 A + I + \eta_2 H + n_3 W\right)}{1+\chi_1 D} - K_3 E\left(S + eV\right)\right) + C_2\left(\tau_1 E - K_4 Q\right) + C_3\left(\theta_1 E - K_5 A\right) + C_4\left(\theta_2 A - K_6 I\right)$$
$$+C_5\left(\theta_3 Q + \tau_2 I - K_7 H\right) - C_6\left(\pi I + \pi\theta H - \varepsilon W\right) \tag{2.16}$$

Since $\frac{S+eV}{1+\chi_1 D} \le S_0 + eV_0 = \frac{P\left(K_2 + ev_1\right)}{K_1 K_2 - v_2 v_1}$ then (2.16) becomes

$$\frac{df}{dt} \le \left(C_3\theta_1 + \tau_1 C_2 - C_1 K_3\left(S_0 + eV_0\right)\right)E + \left(C_5\theta_3 - C_2 K_4\right)Q + \left(C_1\left(S_0 + eV_0\right)\beta\eta_1 + C_4\theta\right)$$
$$\left(C_1\beta\left(S_0 + eV_0\right) - c_4 K_6 + C_6\pi + C_5\tau_2\right)I + \left(C_1\left(S_0 + eV_0\right)\beta\eta_2 + C_6\pi\theta - C_5 K_7\right)H - \tag{2.17}$$
$$\left(C_1\left(S_0 + eV_0\right)\beta\eta_3 - C_6\varepsilon\right)W$$

Substitute (2.14) into (2.17) and with further simplifications to obtain

$$\frac{df}{dt} \le \beta\left(\eta_1 A + I + \eta_2 H + \eta_3 W\right)\left(R_{C1} - 1\right) \tag{2.18}$$

Thus, $\frac{df}{dt} \le 0$ if $R_C \le 1$ with $\frac{df}{dt} = 0$ if and only if $A = I = H = W = 0$. It follows from Lasalle's Invariance Principle (LaSalle & Lefschetz, 1961) that Δ_0 is globally asymptotically stable.

2.6. Bifurcation Analysis

To explore the local stability of the COVID-19 persistent equilibrium Δ_+, bifurcation Analysis will be performed using the centre manifold theory which was described in Castillo-Chavez and Song, (2004) and Akinyemi et al. (2016). To do this, (2.1) is expressed as

$$\frac{dx_1}{dt} = P - \Omega x_1 - K_1 x_1 + v_2 x_2$$
$$\frac{dx_2}{dt} = v_1 x_1 - \Omega e x_2 - K_2 x_2$$
$$\frac{dx_3}{dt} = \Omega\left(x_1 + e x_2\right) - K_3 x_3$$
$$\frac{dx_4}{dt} = \tau_1 x_3 - K_4 x_4$$
$$\frac{dx_5}{dt} = \theta_1 x_3 - K_5 x_5$$
$$\frac{dx_6}{dt} = \theta_2 A - K_6 x_6$$
$$\frac{dx_7}{dt} = \theta_3 x_4 + \tau_2 x_6 - K_7 x_7$$
$$\frac{dx_8}{dt} = l_1 x_5 + l_2 x_6 + l_3 x_7 - \phi x_8$$
$$\frac{dx_9}{dt} = \pi x_6 + \pi\vartheta x_7 - \varepsilon x_9 \qquad (2.19)$$

by replacing $S, V, E, Q, A, I, H, D, W$ with $x_1, x_2, x_3, x_4, x_5, x_6, x_7, x_8, x_9$ respectively, where

$$\Omega = \frac{\beta\left(\eta_1 x_5 + x_6 + \eta_2 x_7 + \eta_3 x_9\right)}{1 + \chi_1 x_8} \qquad (2.20)$$

Supposed $\beta = \beta^*$ is chosen to be the bifurcation parameter when $R_{C1} = 1$ then (2.6) becomes

$$\beta^* = \frac{\varepsilon K_3 K_4 K_5 K_6 K_7}{P A_0\left(\varepsilon K_7 K_4 \theta_1\left(K_6\eta_1 + \theta_2\right) + \varepsilon\eta_2 A_1 + \pi\eta_3 A_2\right)} \qquad (2.21)$$

Let $U = \left(u_1, u_2, u_3, u_4, u_5, u_6, u_7, u_8, u_9\right)$ and $W = \left(w_1, w_2, w_3, w_4, w_5, w_6, w_7, w_8, w_9\right)$ be the corresponding left and right eigen vectors associated with the zero eigen-value of the Jacobian of (2.19) at $\beta = \beta^*$ (denoted by $J_{\beta=\beta^*}$) chosen such that the following conditions are satisfied.

(i) $UJ_{\beta=\beta^*} = 0$

(ii) $J_{\beta=\beta^*} W = 0$

(iii) $UW = 1$

Thus,

$$u_1 = 0,\ u_2 = 0,\ u_8 = 0, \qquad u_3 = \frac{u_6\left(\varepsilon K_7 K_4 \theta_1\left(K_6\eta_1 + \theta_2\right) + \varepsilon\eta_2 A_1 + \pi\eta_3 A_2\right)}{K_3 K_4 K_5\left(\pi\eta_3\left(\vartheta\tau_2 + K_7\right) + \varepsilon\eta_2\tau_2 + \varepsilon K_7\right)},$$

$$u_4 = \frac{u_6 K_6\theta_3\left(\varepsilon\eta_1 + \pi\vartheta\eta_3\right)}{K_4\left(\pi\eta_3\left(\vartheta\tau_2 + K_7\right) + \varepsilon\eta_2\tau_2 + \varepsilon K_7\right)}, \qquad u_7 = \frac{u_6 K_6\left(\varepsilon\eta_1 + \pi\vartheta\eta_3\right)}{\pi\eta_3\left(\vartheta\tau_2 + K_7\right) + \varepsilon\eta_2\tau_2 + \varepsilon K_7}$$

$$u_5 = \frac{u_6\left(\pi\eta_3\theta_2\left(\vartheta\tau_2 + K_7\right) + \varepsilon\eta_2\tau_2\theta_2 + \varepsilon K_7\left(\theta_2 + \eta_1 K_6\right)\right)}{K_5\left(\pi\eta_3\left(\vartheta\tau_2 + K_7\right) + \varepsilon\eta_2\tau_2 + \varepsilon K_7\right)},$$

$$u_9 = \frac{K_6 K\tau\eta_3 u_6}{\left(\pi\eta_3\left(\vartheta\tau_2 + K_7\right) + \varepsilon\eta_2\tau_2 + \varepsilon K_7\right)} \text{ and } u_6 > 0 \text{ free} \qquad (2.22)$$

and

$$w_1 = -\frac{K_3 w_3\left(e\nu_2\nu_1 + K_2^2\right)}{\left(e\nu_1 + K_2\right)\left(K_1 K_2 - \nu_2\nu_1\right)}, \qquad w_2 = -\frac{K_3\nu_1 w_3\left(eK_1 + K_2\right)}{\left(e\nu_1 + K_2\right)\left(K_1 K_2 - \nu_2\nu_1\right)}, \qquad w_4 = \frac{\tau_1 w_3}{K_4}$$

$$w_5 = \frac{\theta_1 w_3}{K_5}, w_6 = \frac{\theta_1\theta_2 w_3}{K_5 K_6}, w_7 = \frac{A_1 w_3}{K_4 K_5 K_6 K_7}, w_8 = \frac{A_3 w_3}{\phi K_4 K_5 K_6 K_7}, w_9 = \frac{A_2\pi w_3}{\varepsilon K_4 K_5 K_6 K_7}$$

and $w_3 > 0$ *free.* (2.23)

The non-zero second-order partial derivatives at Δ_0 associated with (2.19) are given by

$$\frac{\partial^2 f_1}{\partial x_1 \partial x_5} = \frac{\partial^2 f_1}{\partial x_5 \partial x_1} = -\beta\eta_1, \frac{\partial^2 f_1}{\partial x_1 \partial x_6} = \frac{\partial^2 f_1}{\partial x_6 \partial x_1} = -\beta, \frac{\partial^2 f_1}{\partial x_1 \partial x_7} = \frac{\partial^2 f_1}{\partial x_7 \partial x_1} = -\beta\eta_2,$$
$$\frac{\partial^2 f_1}{\partial x_1 \partial x_9} = \frac{\partial^2 f_1}{\partial x_9 \partial x_1} = -\beta\eta_3, \frac{\partial^2 f_2}{\partial x_2 \partial x_5} = \frac{\partial^2 f_2}{\partial x_5 \partial x_2} = -\beta\eta_1 e, \frac{\partial^2 f_2}{\partial x_2 \partial x_6} = \frac{\partial^2 f_2}{\partial x_6 \partial x_2} = -\beta e,$$
$$\frac{\partial^2 f_2}{\partial x_2 \partial x_7} = \frac{\partial^2 f_2}{\partial x_7 \partial x_2} = -\beta\eta_2 e, \frac{\partial^2 f_2}{\partial x_2 \partial x_9} = \frac{\partial^2 f_2}{\partial x_9 \partial x_2} = -\beta\eta_3 e, \frac{\partial^2 f_3}{\partial x_1 \partial x_5} = \frac{\partial^2 f_3}{\partial x_5 \partial x_1} = \beta\eta_1$$
$$\frac{\partial^2 f_3}{\partial x_1 \partial x_6} = \frac{\partial^2 f_3}{\partial x_6 \partial x_1} = \beta, \frac{\partial^2 f_3}{\partial x_1 \partial x_7} = \frac{\partial^2 f_3}{\partial x_7 \partial x_1} = \beta\eta_2, \frac{\partial^2 f_3}{\partial x_1 \partial x_9} = \frac{\partial^2 f_3}{\partial x_9 \partial x_1} = \beta\eta_3,$$
$$\frac{\partial^2 f_3}{\partial x_2 \partial x_5} = \frac{\partial^2 f_3}{\partial x_5 \partial x_2} = \beta\eta_1 e, \frac{\partial^2 f_3}{\partial x_2 \partial x_6} = \frac{\partial^2 f_3}{\partial x_6 \partial x_2} = \beta e, \frac{\partial^2 f_3}{\partial x_2 \partial x_7} = \frac{\partial^2 f_3}{\partial x_7 \partial x_2} = \beta\eta_2 e$$
$$\frac{\partial^2 f_3}{\partial x_2 \partial x_9} = \frac{\partial^2 f_2}{\partial x_9 \partial x_2} = \beta\eta_3 e, \frac{\partial^2 f_1}{\partial x_8 \partial x_9} = \frac{\partial^2 f_1}{\partial x_9 \partial x_8} = \frac{\beta\eta_3 P K_2 \chi_1}{\mu(K_2 + v_1)},$$
$$\frac{\partial^2 f_3}{\partial x_8 \partial x_9} = \frac{\partial^2 f_3}{\partial x_9 \partial x_8} = -\frac{\beta\eta_3 P \chi_1 (e v_1 + K_2)}{\mu(K_2 + v_1)}, \frac{\partial^2 f_1}{\partial x_8 \partial x_5} = \frac{\partial^2 f_1}{\partial x_5 \partial x_8} = \frac{\beta\eta_1 P K_2 \chi_1}{\mu(K_2 + v_1)},$$
$$\frac{\partial^2 f_2}{\partial x_8 \partial x_5} = \frac{\partial^2 f_2}{\partial x_5 \partial x_8} = \frac{\beta\eta_1 P e v_1 \chi_1}{\mu(K_2 + v_1)}, \frac{\partial^2 f_3}{\partial x_8 \partial x_5} = \frac{\partial^2 f_3}{\partial x_5 \partial x_8} = \frac{-\beta\eta_1 P \chi_1 (e v_1 + K_2)}{\mu(K_2 + v_1)},$$
$$\frac{\partial^2 f_3}{\partial x_8 \partial x_6} = \frac{\partial^2 f_3}{\partial x_6 \partial x_8} = \frac{-\beta P \chi_1 (e v_1 + K_2)}{\mu(K_2 + v_1)}, \frac{\partial^2 f_1}{\partial x_8 \partial x_6} = \frac{\partial^2 f_1}{\partial x_6 \partial x_8} = \frac{\beta P K_2 \chi_1}{\mu(K_2 + v_1)},$$
$$\frac{\partial^2 f_2}{\partial x_8 \partial x_6} = \frac{\partial^2 f_2}{\partial x_6 \partial x_8} = \frac{\beta P e v_1 \chi_1}{\mu(K_2 + v_1)}, \frac{\partial^2 f_3}{\partial x_8 \partial x_7} = \frac{\partial^2 f_3}{\partial x_7 \partial x_8} = \frac{-\beta\eta_2 P \chi_1 (e v_1 + K_2)}{\mu(K_2 + v_1)} \quad (2.24)$$
$$\frac{\partial^2 f_1}{\partial x_8 \partial x_7} = \frac{\partial^2 f_1}{\partial x_7 \partial x_8} = \frac{\beta\eta_2 P \chi_1}{\mu(K_2 + v_1)}, \frac{\partial^2 f_2}{\partial x_8 \partial x_7} = \frac{\partial^2 f_2}{\partial x_7 \partial x_8} = \frac{\beta\eta_2 P e v_1 \chi_1}{\mu(K_2 + v_1)}$$
$$\frac{\partial^2 f_2}{\partial x_8 \partial x_9} = \frac{\partial^2 f_2}{\partial x_9 \partial x_8} = \frac{\beta\eta_3 P e v_1 \chi_1}{\mu(K_2 + v_1)}$$

and

$$\frac{\partial^2 f_1}{\partial x_5 \partial \beta} = \frac{\partial^2 f_1}{\partial \beta \partial x_5} = \frac{-\eta_1 P K_2}{\mu(K_2+v_1)}, \frac{\partial^2 f_2}{\partial x_5 \partial \beta} = \frac{\partial^2 f_2}{\partial \beta \partial x_5} = \frac{-\eta_1 P e v_1}{\mu(K_2+v_1)},$$
$$\frac{\partial^2 f_1}{\partial x_6 \partial \beta} = \frac{\partial^2 f_1}{\partial \beta \partial x_6} = \frac{-P K_2}{\mu(K_2+v_1)}, \frac{\partial^2 f_2}{\partial x_6 \partial \beta} = \frac{\partial^2 f_2}{\partial \beta \partial x_6} = \frac{-P e v_1}{\mu(K_2+v_1)},$$
$$\frac{\partial^2 f_3}{\partial x_5 \partial \beta} = \frac{\partial^2 f_3}{\partial \beta \partial x_5} = \frac{\eta_1 P(K_2+e v_1)}{\mu(K_2+v_1)}, \frac{\partial^2 f_3}{\partial x_6 \partial \beta} = \frac{\partial^2 f_3}{\partial \beta \partial x_6} = \frac{P(K_2+e v_1)}{\mu(K_2+v_1)}$$
$$\frac{\partial^2 f_1}{\partial x_7 \partial \beta} = \frac{\partial^2 f_1}{\partial \beta \partial x_7} = \frac{-\eta_2 P K_2}{\mu(K_2+v_1)}, \frac{\partial^2 f_2}{\partial x_7 \partial \beta} = \frac{\partial^2 f_2}{\partial \beta \partial x_7} = \frac{-\eta_2 P e v_1}{\mu(K_2+v_1)},$$
$$\frac{\partial^2 f_3}{\partial x_5 \partial \beta} = \frac{\partial^2 f_3}{\partial \beta \partial x_5} = \frac{\eta_1 P(K_2+e v_1)}{\mu(K_2+v_1)}, \frac{\partial^2 f_3}{\partial x_7 \partial \beta} = \frac{\partial^2 f_3}{\partial \beta \partial x_7} = \frac{\eta_2 P(K_2+e v_1)}{\mu(K_2+v_1)}$$
$$\frac{\partial^2 f_1}{\partial x_9 \partial \beta} = \frac{\partial^2 f_1}{\partial \beta \partial x_9} = \frac{-\eta_3 P K_2}{\mu(K_2+v_1)}, \frac{\partial^2 f_2}{\partial x_9 \partial \beta} = \frac{\partial^2 f_2}{\partial \beta \partial x_9} = \frac{-\eta_3 P e v_1}{\mu(K_2+v_1)},$$
$$\frac{\partial^2 f_3}{\partial x_9 \partial \beta} = \frac{\partial^2 f_3}{\partial \beta \partial x_9} = \frac{\eta_3 P(K_2+e v_1)}{\mu(K_2+v_1)}. \tag{2.25}$$

Using (2.22)-(2.25) such that $n=9$ to compute a and b as defined in Castillo-Chavez and Song (2004) to get

$$a = \frac{-2\beta u_3(w_5\eta_1 + w_7\eta_2 + w_9\eta_3 + w_6)}{\mu(K_2+v_1)}\left(P w_8 \chi_1 - \mu(e w_2 + w_1)\right)(e v_1 + K_2) \tag{2.26}$$

and

$$b = \frac{u_3(w_5\eta_1 + w_7\eta_2 + w_9\eta_3 + w_6)}{\mu(K_2+v_1)}(e v_1 + K_2) \tag{2.27}$$

It is obvious to note that $b>0$ and $a<0$ since all the parameters values are positive and since $w_1<0$ and $w_2<0$. Thus, (1.1) exhibits forward bifurcation if $R_{C1}>1$ and the next result is obtained.

Theorem 3. The unique COVID-19 persistent equilibrium for model (1.1) is locally asymptotically stable if $R_{C1}>1$ and is close to unity.

2.7 Sensitivity Analysis

Sensitivity analysis is carried out using the normalized forward sensitivity index of the reproduction number R_{C1} as discussed in Akinyemi et al. 2023, to investigate the effects of changes in parameter values on the spread of COVID-19. Maple 18 software is used to get the sensitivity indices presented in Table 4.1.

$$\Theta_{\alpha_1}^{R_{C1}} = \frac{\partial R_{C1}}{\partial \alpha_1} \times \frac{\alpha_1}{R_{C1}} = -0.01656; \quad \Theta_{\eta_2}^{R_{C1}} = \frac{\partial R_{C1}}{\partial \eta_2} \times \frac{\eta_2}{R_{C1}} = +0.0782; \quad \Theta_{\eta_3}^{R_{C1}} = \frac{\partial R_{C1}}{\partial \eta_3} \times \frac{\eta_3}{R_{C1}} = +0.0012;$$

$$\Theta_{\beta}^{R_{C1}} = \frac{\partial R_{C1}}{\partial \beta} \times \frac{\beta}{R_{C1}} = +0.9288; \quad \Theta_{\alpha_2}^{R_{C1}} = \frac{\partial R_{C1}}{\partial \alpha_2} \times \frac{\alpha_2}{R_{C1}} = -0.0644; \quad \Theta_{\alpha_3}^{R_{C1}} = \frac{\partial R_{C1}}{\partial \alpha_3} \times \frac{\alpha_3}{R_{C1}} = -0.0737;$$

$$\Theta_{\theta_1}^{R_{C1}} = \frac{\partial R_{C1}}{\partial \theta_1} \times \frac{\theta_1}{R_{C1}} = +0.0123; \quad \Theta_{\theta_2}^{R_{C1}} = \frac{\partial R_{C1}}{\partial \theta_2} \times \frac{\theta_2}{R_{C1}} = +0.0410; \quad \Theta_{\theta_3}^{R_{C1}} = \frac{\partial R_{C1}}{\partial \theta_3} \times \frac{\theta_3}{R_{C1}} = +0.000004;$$

$$\Theta_{\phi}^{R_{C1}} = \frac{\partial R_{C1}}{\partial \phi} \times \frac{\phi}{R_{C1}} = 0; \quad \Theta_{\nu_2}^{R_{C1}} = \frac{\partial R_{C1}}{\partial \nu_2} \times \frac{\nu_2}{R_{C1}} = \quad +0.2235; \quad \Theta_{\tau_1}^{R_{C1}} = \frac{\partial R_{C1}}{\partial \tau_1} \times \frac{\tau_1}{R_{C1}} = -0.0122;$$

$$\Theta_{\tau_2}^{R_{C1}} = \frac{\partial R_{C1}}{\partial \tau_2} \times \frac{\tau_2}{R_{C1}} = -0.230; \quad \Theta_{\chi_1}^{R_{C1}} = \frac{\partial R_{C1}}{\partial \chi_1} \times \frac{\chi_1}{R_{C1}} = 0; \quad \Theta_{\nu_1}^{R_{C1}} = \frac{\partial R_{C1}}{\partial \nu_1} \times \frac{\nu_1}{R_{C1}} = +0.2236;$$

$$\Theta_{\eta_1}^{R_{C1}} = \frac{\partial R_{C1}}{\partial \eta_1} \times \frac{\eta_1}{R_{C1}} = +0.2576; \quad \Theta_{\Pi}^{R_{C1}} = \frac{\partial R_{C1}}{\partial \Pi} \times \frac{\Pi}{R_{C1}} = +0.0012; \quad \Theta_{\vartheta}^{R_{C1}} = \frac{\partial R_{C1}}{\partial \vartheta} \times \frac{\vartheta}{R_{C1}} = +0.0001;$$

$$\Theta_{\varepsilon}^{R_{C1}} = \frac{\partial R_{C1}}{\partial \varepsilon} \times \frac{\varepsilon}{R_{C1}} = -0.0012 \tag{4.49}$$

Table 4.1: Sensitivity Analysis Results

Parameter	Sensitivity index of R_{C1} wrt $v\left(\Theta_{v}^{R_{C1}}\right)$
θ_1	+0.0123
θ_2	+0.0410
θ_3	+0.000004
τ_1	–0.0122
τ_2	–0.230
α_1	–0.1656
α_2	–0.00644
α_3	–0.0737
ν_1	–0.2236
ν_2	+0.2235
χ_1	0
η_1	+0.2576
η_2	+0.0782
η_3	+0.0012
β	+0.9288
π	0.0012

ϑ	+0.0001
ε	–0.0012
ϕ	0

3.0 Numerical Simulation

To validate the qualitative results presented in Section 2, we shall make use of the value of parameters and the initial condition in Usman et al. (2023).

The effect of varying the initial population of (1.1) for different equilibrium points is shown in Figures 3.1-3.6. In Fig 3.1, the variation of the population of all infected individuals converges to zero when $R_{C1} = 0.6918 < 1$

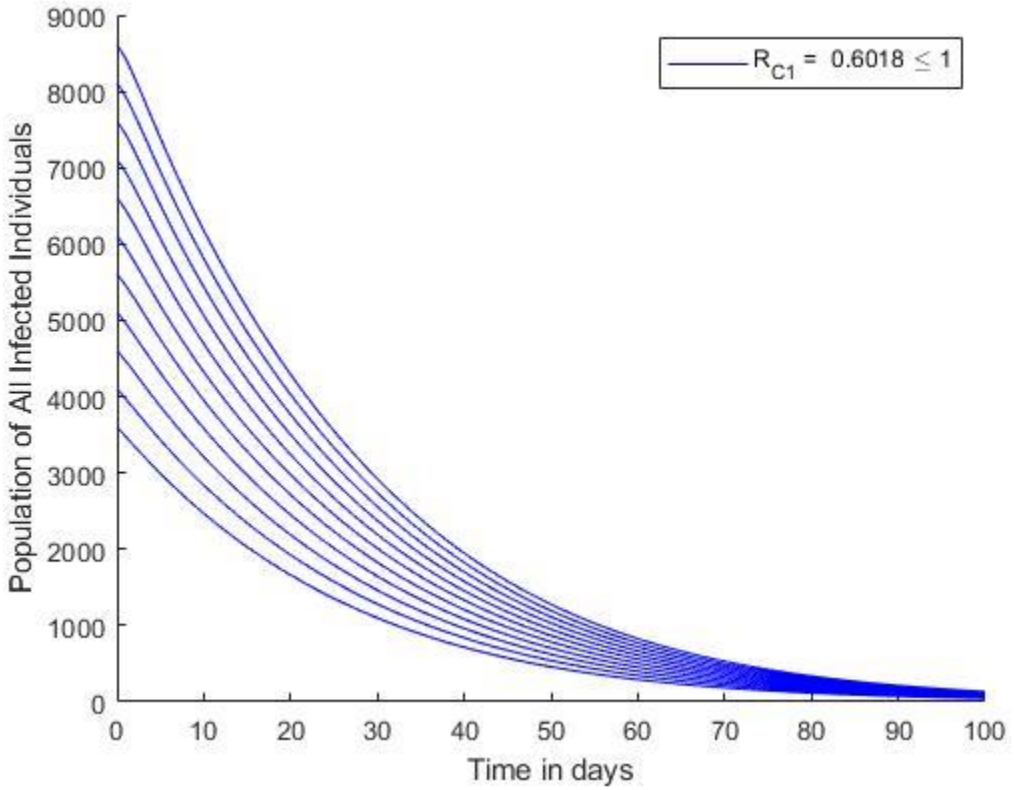

Figure 3.1: Convergence of solution trajectories for all infected humans when $R_{C1} = 0.6918 < 1$.

Fig 3.2, the variation of the initial population of COVID-19 deceased individuals tends to zero when $R_{C1} = 0.6918 < 1$.

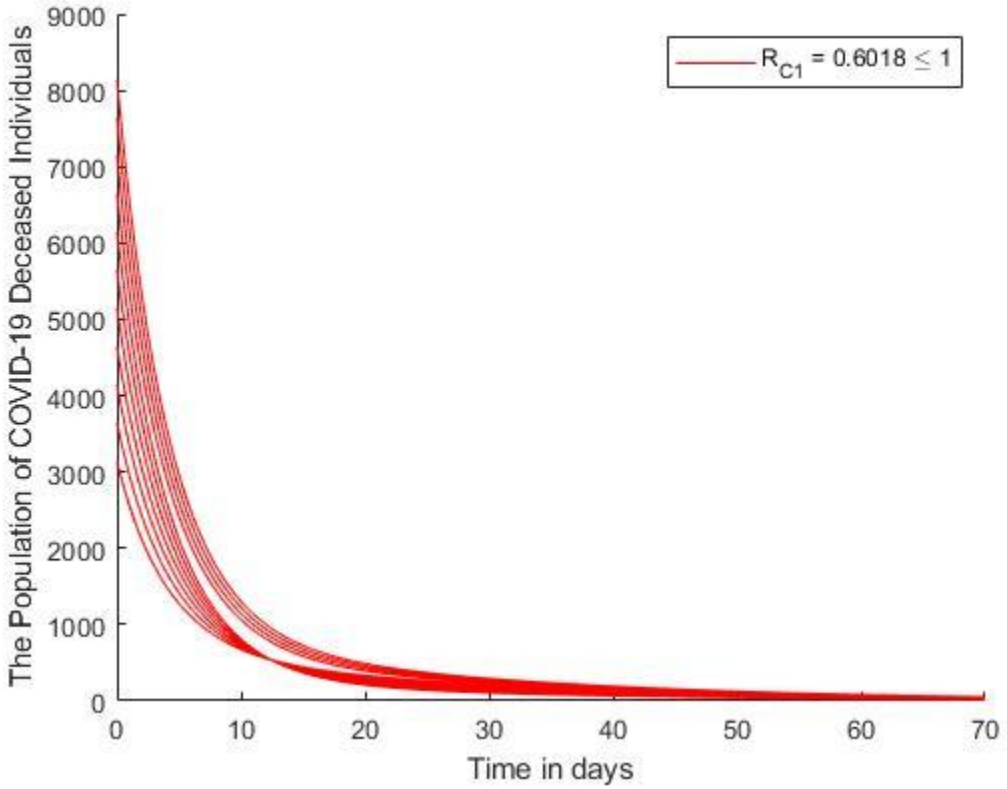

Figure 3.2: Convergence of solution trajectories for COVID-19 deceased individuals when $R_{C1} = 0.6918 < 1$

The initial concentration of COVID-19 viruses in the environment is varied in Fig. 3.3 and converges to zero at $R_{C1} = 0.6918 < 1$.

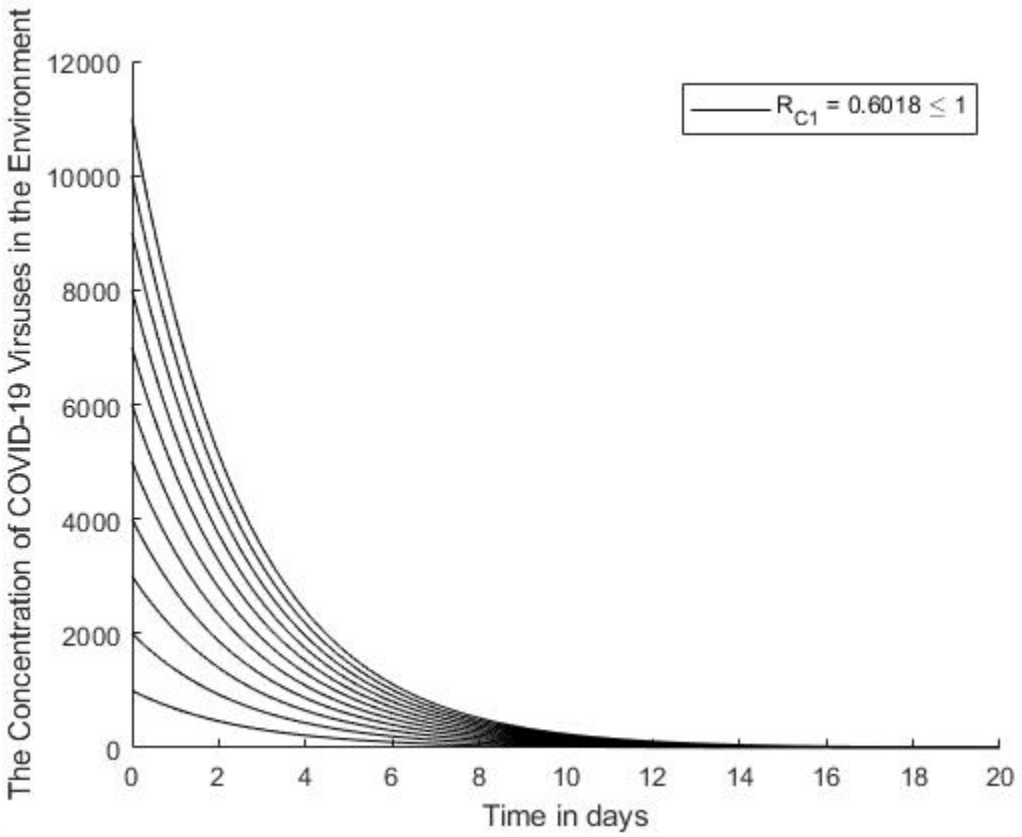

Figure 3.3: Convergence of solution trajectories for COVID-19 Viruses in the environment when $R_{C1} = 0.6918 < 1$.

It is important to note that Fig. 3.1-3.3 validates the global stability result for the CFE of (1.1) presented by Theorem 2. Fig.3.4 shows that irrespective of the initial population of all infected individuals, It converges to $E_+ + A_+ + Q_+ + I_+ + H_+$ provided $R_{C1} = 1.2035 > 1$.

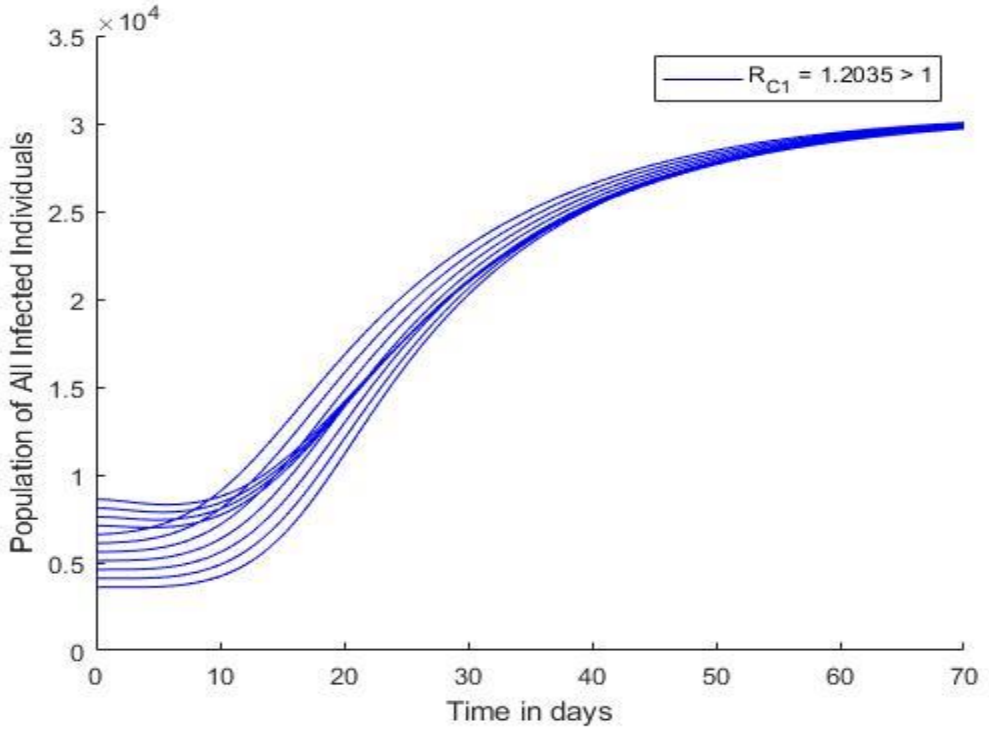

Figure 3.4: Convergence of solution trajectories for all infected humans when $R_{C1} = 1.2035 > 1$

Similarly, Fig.3.5 shows that irrespective of the initial population of COVID-19 deceased individuals, the population of COVID-19 deceased individuals converges to D_+ provided $R_{C1} = 1.2035 > 1$.

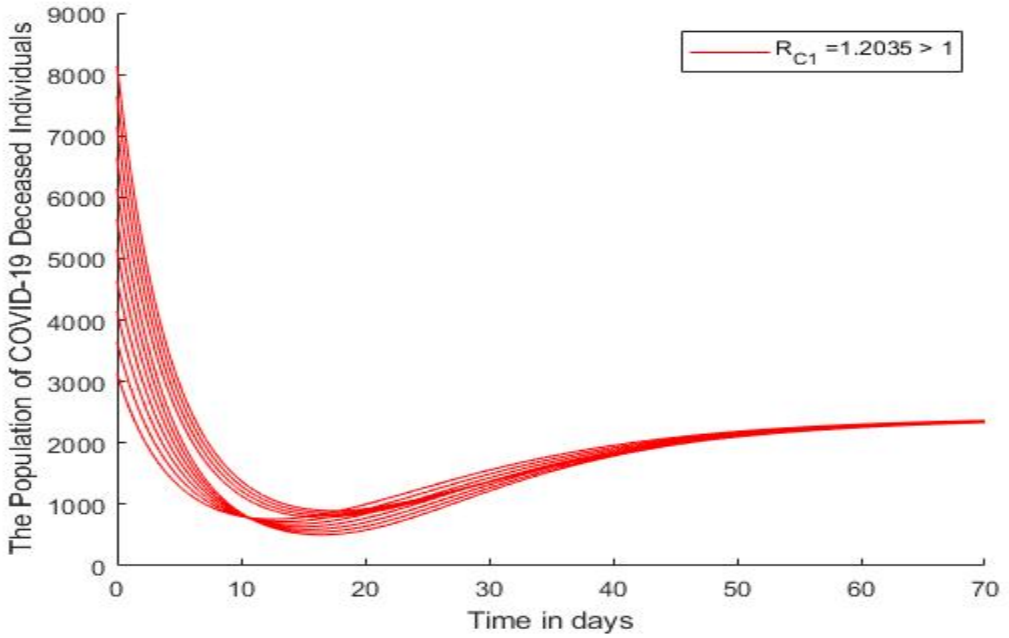

Figure 3.5: Convergence of solution trajectories for COVID-19 deceased individuals when $R_{C1} = 1.2035 > 1$

Fig. 3.6 shows that provided $R_{C1} = 1.2035 > 1$, the concentration of COVID-19 viruses in the environment converges to W_+ irrespective of the initial concentration.

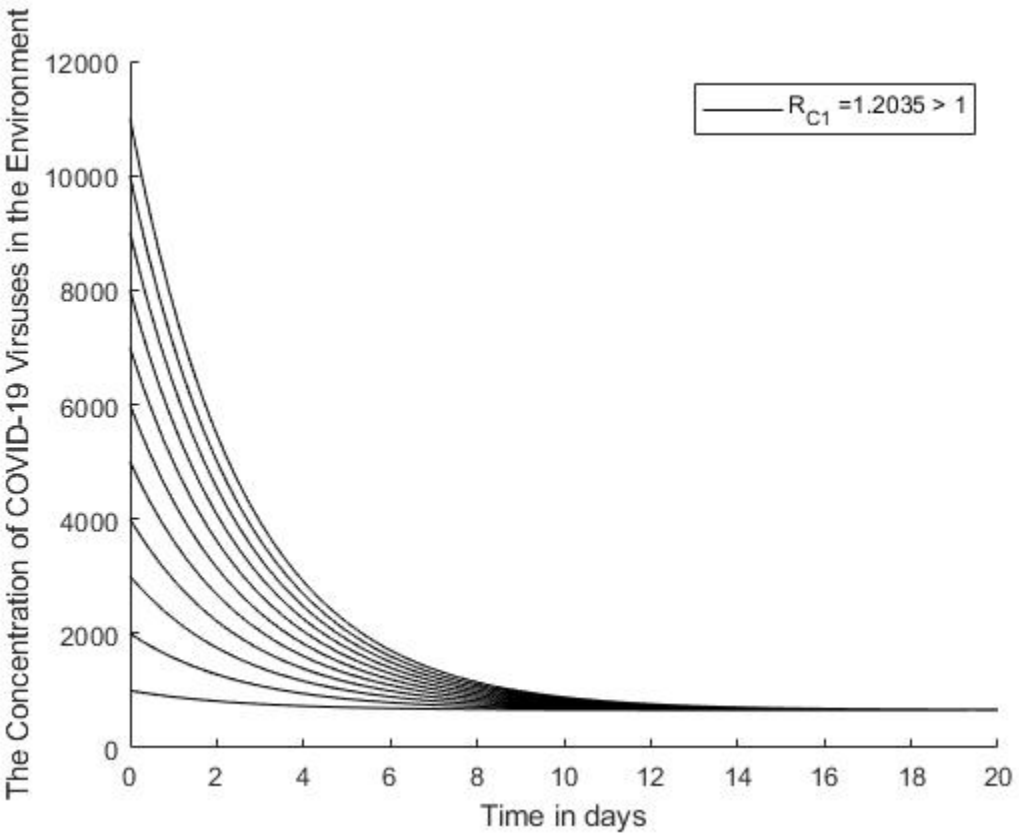

Figure 3.6: Convergence of solution trajectories for COVID-19 Viruses in the Environment when $R_{C1} = 1.2035 > 1$

The numerical simulation displayed in Fig. 3.4-3.6 establishes that the CPE of (1.1) is globally asymptotically stable when the $RC1 = 1.2035 > 1$.

3.1 Simulation for χ_1

The impact of the fear of COVID-19 infection on the transmission dynamics of COVID-19 is, investigated through numerical simulation. This is done by comparing the following five fear levels, namely, no fear ($\chi_1 = 0$), low fear level ($\chi_1 = 0.25$), moderate fear level ($\chi_1 = 0.5$), high fear level ($\chi_1 = 0.75$) and very high fear level ($\chi_1 = 1$). Fig. 3.7 shows the impact of different levels of fear associated with COVID-19 infection on the population of all infected humans. Fig. 3.7a shows that in the absence of fear ($\chi_1 = 0$) associated with COVID-19 infection, there are more COVID-19-infected humans compared to when the fear level is low ($\chi_1 = 0.25$). Fig. 3.7b reveals that as the level of fear of COVID-19 infection increases the number of infected humans decreases. This means that as the general public becomes more scared of being infected, there will be a decline in the number of humans with COVID-19 infection. The epidemiological implication of this finding is that the populace will adhere to public

health measures to avoid being infected. Thus, this agrees with the findings of Murad et al. (2022), Karlsson et al. (2021) and Recio-Vivas et al. (2020).

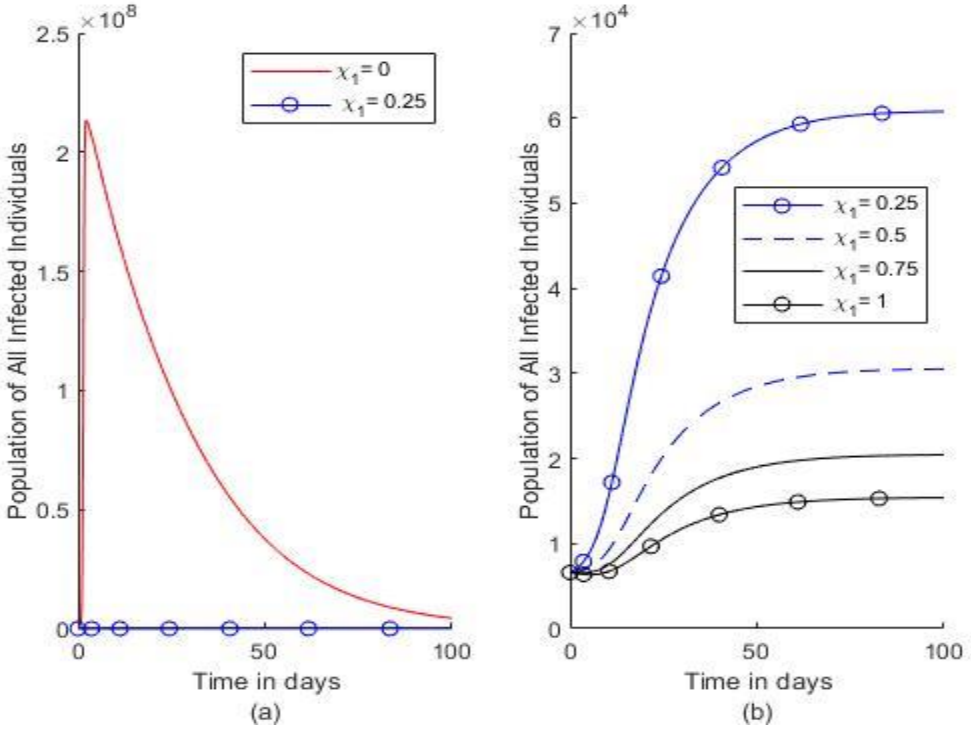

Figure 3.7:Impact of Varying χ_1 on the Population of All Infected Individuals

The impact of the various levels of fear associated with COVID-19 infection on the population of COVID-19 deceased individuals are shown in Fig. 3.8. Fig. 3.8a shows that there are more COVID-19 induced death cases in the absence of fear ($\chi_1 = 0$) as compared to when the fear level is low ($\chi_1 = 0.25$). Fig. 3.8b conveys that the decrease in χ_1 implies an increase on the number of COVID-19 induced death cases.

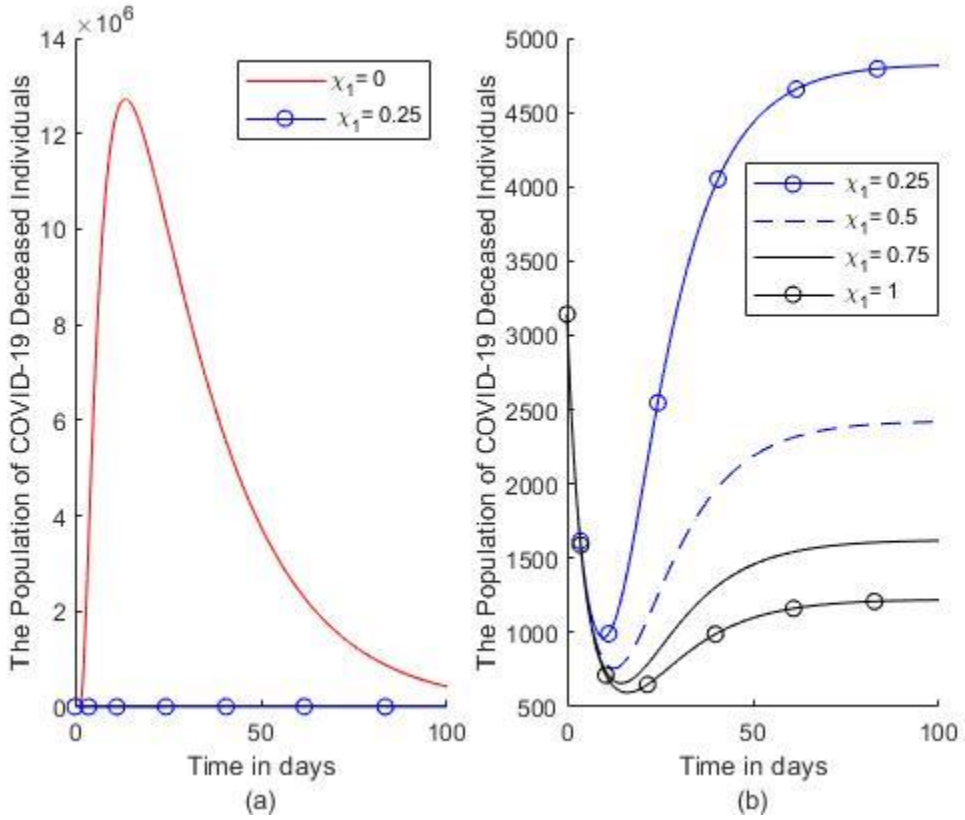

Figure 3.8: Variation of χ_1 on the Population of COVID-19 Deceased Individuals

The effect of varying χ_1 on the concentration of COVID-19 viruses in the environment is displayed in Fig. 3.9. Similarly, Fig. 3.9a and Fig. 3.9b shows that an increase in χ_1 yields decrease in the concentration of COVID-19.

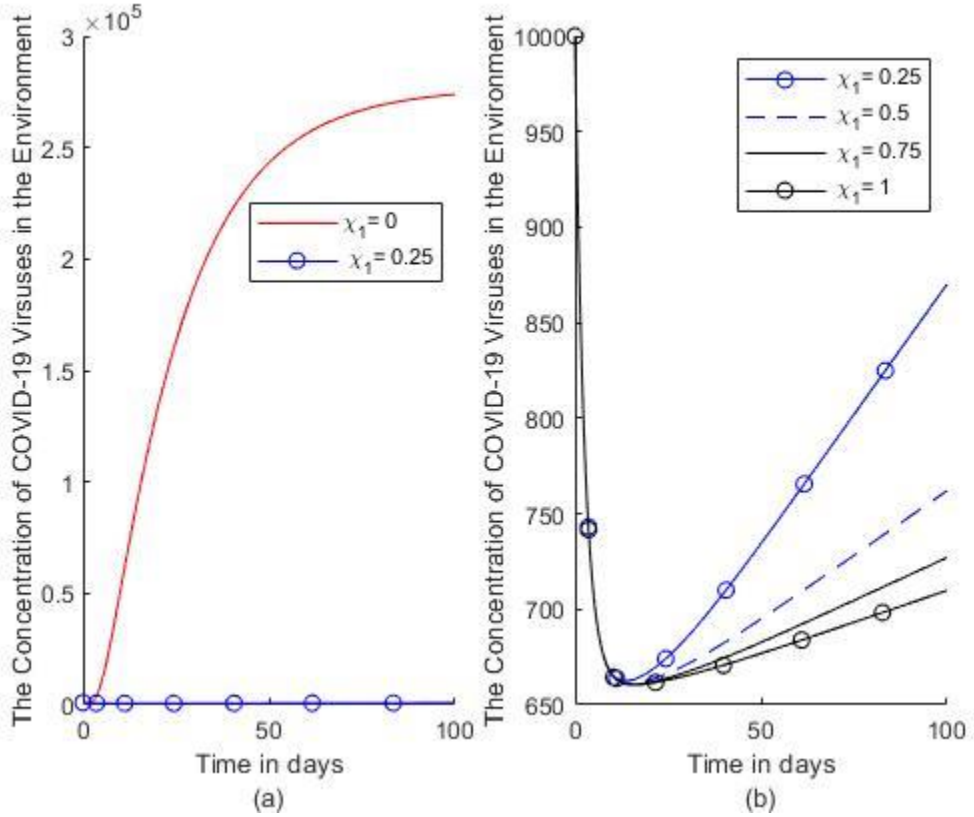

Figure 3.9: Impact of Varying χ_1 on the Concentration of COVID-19 Viruses

4.0 Conclusion

This study presents the qualitative analysis of the COVID-19 mathematical model coupled with the fear of infection in Usman et al., 2023. The two equilibrium points (i.e. the CFE and CPE) of the model were found and the reproduction number (R_{C1}) for the model was computed using the next-generation matrix method. This study further shows that the CPE is locally asymptotically stable when R_{C1} is above unity and the CFE is globally asymptotically stable for less than one. The model is also shown to exhibit forward bifurcation, thus the threshold is sufficient to control the spread of COVID-19. Sensitivity analysis suggests that fear of infection does not influence the R_{C1} but the numerical simulation reveals that as the level of fear of infection increases, the population of all infected humans, COVID-19 deceased individuals and the concentration of the COVID-19 virus increases.

References

Akinyemi, S.T., Ibrahim, M.O. and Edogbanya, H.O. (November, 2016). Stability and Bifurcation Analysis of Ebola Deterministic Model. *National Mathematical Centre (NMC): Journal of Mathematical Sciences*, **2**(1):803-820.

Akinyemi, S. T., Ibrahim, M. O., Usman, I. G., & Odetunde, O. (2016). Global stability analysis of sir epidemic model with relapse and immunity loss. *International Journal of Applied Science and Mathematical Theory*,2(1),1-14.

Akinyemi, S. T., Idisi, I. O., Rabiu, M., Okeowo, V. I., Iheonu, N., Dansu, E. J., ... & Oshinubi, K. (2023).A tale of two countries: optimal control and cost-effectiveness analysis of monkeypox disease in Germany and Nigeria. *Healthcare Analytics*, 4(100258),1-26.

Altier, M. B. (2023). Criminal or terrorist? Fear, bias, and public support for prisoner reentry programs. Terrorism and Political Violence, 35(1), 83-103.

Amanna, I., & Slifka, M. K. (2005). Public fear of vaccination: separating fact from fiction. *Viral immunology*, 18(2): 307-315.

Benavente, J. M., & Goya, D. (2023). The fear-increasing and fear-decreasing effects of a pilot policy to reduce fear of crime. *Plos One*, 18(3), 1-16.

Bendau, A., Plag, J., Petzold, M. B., & Stro¨hle, A. (2021). COVID-19 vaccine hesitancy and related fears and anxiety.*International immunopharmacology*, 97, 1-5.

Bove, V., Elia, L., & Ferraresi, M. (2023). Immigration, Fear of Crime, and Public Spending on Security. *The Journal of Law, Economics, and Organization*, 39(1), 235-280.

Castillo-Chavez, C., & Song, B. (2004). Dynamical models of tuberculosis and their applications. Math. Biosci. Eng, 1(2), 361-404.

Colonnello, V., Leonardi, G., Farinelli, M., Bertoletti, E., & Russo, P. M. (2023). Psychological distress in hospitalized patients without COVID-19 symptoms: the role of fear of infection and remote contact with informal caregivers. *Psychological Medicine*, 53(1), 297-298.

Elmojtaba, I., Al-Yahyai, M., Al-Ghassani, A., Al-Musalhi, F., & Al-Salti, N. (2023, June). Investigating the role of environmental transmission in COVID-19 Dynamics: a mathematical model Based Study. In *AIP Conference Proceedings* (Vol. 2781, No. 1). AIP Publishing.

Falco-Gimeno, A., Mu ´ noz, J., & Pannico, R. (2023). Double-edged bullets: the conditional effect of terrorism on vote for the incumbent. *British Journal of Political Science*, 53(1), 183-203.

Ilesanmi, O., & Afolabi, A. (2020). Perception and practices during the COVID-19 pandemic in an urban community in Nigeria: a cross-sectional study. *PeerJ*, 8,1-15.

James, T. O., Akinyemi, S. T., & Oluwade, B. (2015). Stability analysis of Lassa fever with quarantine and permanent immunity. *International Journal of Applied Science and Mathematical Theory*, 1(8),71-81.

Johnston, M. D., & Pell, B. (2020). A dynamical framework for modeling fear of infection and frustration with social distancing in COVID-19 spread. *Mathematical Biosciences and Engineering*, 17(6), 7892-7915.

Karlsson, L. C., Soveri, A., Lewandowsky, S., Karlsson, L., Karlsson, H., Nolvi, S., &Antfolk, J. (2021). Fearing the disease or the vaccine: The case of COVID-19. *Personality and individual differences*, 172(4), 110-124.

Kaskeleviciute, R., Knupfer, H., & Matthes, J. (2023). See something, say something? The role of online self-disclosure on fear of terror among young social media users. *New Media & Society*,00(0): 1-29.

Kroesen, M., De Vos, J., Le, H. T., & Ton, D. (2023). Exploring attitudebehaviour dynamics during COVID-19: How fear of infection and working from home influence train use and the attitude toward this mode. *Transportation Research Part A: Policy and Practic*e, 167:1-12.

LaSalle, J. P. and S. Lefschetz, S. (1961). *Stability by Liapunov's Direct Method*, with Applications, Academic Press, New York

Makinde, O. D. (2007). Adomian decomposition approach to a SIR epidemic model with constant vaccination strategy. *Applied Mathematics and Computation*, 184(2), 842-848.

Malas, O., & Tols*a´*, M. D. (2021). Vaccination Fear Scale (VFS-6): Development and Initial Validation. *Mediterranean Journal of Clinical Psychology*, 9(2),1-19.

Mondal, N., Barman, D., Roy, J., Alam, S., & Sajid, M. (2023). A Modified Leslie-Gower Fractional Order Prey-Predator Interaction Model Incorporating The Effect Of Fear On Prey.*Journal of Applied Analysis & Computation*, 13(1), 198-232.

Mpeshe, S. C., & Nyerere, N. (2021). Modeling the dynamics of coronavirus disease pandemic coupled with fear epidemics. *Computational and Mathematical Methods in Medicine*, 2021:1-9.

Murad, O., Al-Dassean, K. A., Al Neweiri, A. M., Murad, H. O., & Murad,B. O. (2022). The Arabic version of the fear of covid-19 scale: psychometric properties and relationship to future anxiety in Jordanians. *Cogent Psychology*, 9(1), 2064730.

Odetunde, O., Ibrahim, M. O., Olotu, O. T., Uwaheren, O. A., & Akinyemi, S. T. (2022). Stability and bifurcation analysis of COVID-19 mathematical model incorporating case detection. *Malaysian Journal of Computing*, *7*(1), 952-967.

Okoye, C., Collins, O. C., & Mbah, G. C. E. (2023). Mathematical approach to the analysis of terrorism dynamics. *In Ten Years of Boko Haram in Nigeria: The Dynamics and Counterinsurgency Challenges (pp. 95-106). Cham: Springer Nature Switzerland*.

Pratama, R. A., Loupatty, M., Hariyanto, H., Caesarendra, W., & Rahmaniar, W. (2023). Fear and Group Defense Effect of a Holling Type IV Predator-Prey System Intraspecific Competition. *Emerging Science Journal*, 7(2): 385-395.

Rashid, S., & Jarad, F. (2023). Stochastic dynamics of the fractal-fractional Ebola epidemic model combining a fear and environmental spreading mechanism. *AIMS Mathematics*, 8(2), 3634-3675.

Recio-Vivas, A. M., Font-Jimenez, I., Mansilla-Dom ´ *A*˜nguez, J. M., BelzuneguiEraso, A., D´ıaz-Perez, D., Lorenzo-Allegue, L., & Pe ´ na-Otero, D. (2022). Fear and attitude towards SARS-CoV-2 (COVID-19) Infection in Spanish population during the period of confinement. *International Journal of Environmental Research and Public Health*, 19(2), 834.

Rodr´ıguez-Hidalgo, A. J., Pantaleon, Y., Dios, I., & Falla, D. (2020). Fear ´of COVID-19, stress, and anxiety in university undergraduate students: a predictive model for depression. *Frontiers in psychology*, 11, 591797.

Sato, R., & Fintan, B. (2020). Fear, knowledge, and vaccination behaviors among women in Northern Nigeria. *Human Vaccines & Immunotherapeutics*, 16(10): 2438-2448.

Shanafelt, T., Ripp, J., & Trockel, M. (2020). Understanding and addressing sources of anxiety among health care professionals during the COVID-19 pandemic. *Jama*, 323(21), 2133-2134.

Tang, Y. M., Wu, T. L., & Liu, H. T. (2023). Causal Model Analysis of the Effect of Formalism, Fear of Infection, COVID-19 Stress on Firefighters? Post-Traumatic Stress Syndrome and Insomnia. *International Journal of Environmental Research and Public Health*, 20(2):1-15.

Thirthar, A. A., Abboubakar, H., Khan, A., & Abdeljawad, T. (2023). Mathematical modeling of the COVID-19 epidemic with fear impact. *AIMS Mathematics*, 8(3), 6447-6465.

Usman, I. G., Ibrahim, M. O., Isah, B. Y., Lawal, N., & Akinyemi, S. T. (2023). Application of NonStandard Finite Difference Method on Covid-19 Mathematical Model with Fear of Infection. *Fudma Journal of Sciences*, 7(4), 357-368.

Van den Driessche, P. (2008). Deterministic compartmental models: extensions of basic models. *Mathematical epidemiology*, 147-157.

Yousaf, M., Afzaal, M., DarAssi, M. H., Khan, M. A., Alshahrani, M. Y., & Suliman, M. (2022). A Mathematical Model of Vaccinations Using New Fractional Order Derivative. *Vaccines*, 10(12), 1980.

Yousef, A., Bozkurt, F., Abdeljawad, T., & Emreizeeq, E.(2023). A mathematical model of COVID-19 and the multi fears of the community during the epidemiological stage. *Journal of Computational and Applied Mathematics*, 419, 1-17.

Zhao, J., & Shao, Y. (2023). Bifurcations of a prey-predator system with fear, refuge and additional food. *Mathematical Biosciences and Engineering*, 20(2), 3700-3720.